Journal of Statistical Physics, Vol. 118, Nos. 5/6, March 2005 (© 2005)
DOI: 10.1007/s10955-004-2022-0

Infinite Compressibility States in the Hierarchical Reference Theory of Fluids. II. Numerical Evidence

Albert Reiner[1,2] **and Gerhard Kahl**[1]

Received August 18, 2004; accepted September 30, 2004

Continuing our investigation into the Hierarchical Reference Theory of fluids for thermodynamic states of infinite isothermal compressibility κ_T we now turn to the available numerical evidence to elucidate the character of the partial differential equation: Of the three scenarios identified previously, only the assumption of the equations turning stiff when building up the divergence of κ_T allows for a satisfactory interpretation of the data. In addition to the asymptotic regime where the arguments of part I directly apply, a similar mechanism is identified that gives rise to transient stiffness at intermediate cutoff for low enough temperature. Heuristic arguments point to a connection between the form of the Fourier transform of the perturbational part of the interaction potential and the cutoff where finite difference approximations of the differential equation cease to be applicable, and they highlight the rather special standing of the hard-core Yukawa potential as regards the severity of the computational difficulties.

KEY WORDS: Liquid-vapor transitions; non-linear partial differential equations; numerical analysis; finite differences; stiffness.

1. INTRODUCTION

Building upon the results of part I[(1)], q. v., and maintaining the notational and semantic conventions introduced there, we now turn to the numerical solution of the HRT PDE[(2–8)]

$$\frac{\partial f}{\partial Q} = d_{00} + d_{02}\,\frac{\partial^2 f}{\partial \rho^2} \tag{1}$$

[1]Institut für Theoretische Physik and Center for Computational Materials Science, Technische Universität Wien, Wiedner Hauptstraße 8–10, A–1040 Vienna, Austria.
[2]Teoretisk fysikk, Institutt for fysikk, Norges teknisk-naturvitenskapelige universitet Trondheim, Høgskoleringen 5, N–7491 Trondheim, Norway; e-mail: areiner@tph.tuwien.ac.at

in order to determine the type of behavior that actually occurs in practical applications of the theory for thermodynamic states of diverging isothermal compressibility κ_T. To this end, we consider two simple model potentials $v(r) = v^{\text{hs}}(r) + w(r)$, viz., the hard-core Yukawa (HCY) system,

$$w^{\text{hcy}}(r) = \begin{cases} -\epsilon_0 & : r < \sigma \\ -\epsilon \frac{\sigma}{r} e^{-z(r-\sigma)} & : r > \sigma, \end{cases} \tag{2}$$

and square wells (SWs),

$$w^{\text{sw}}(r) = \begin{cases} -\epsilon & : r < \lambda\sigma \\ 0 & : r > \lambda\sigma, \end{cases} \tag{3}$$

to illustrate the types of behavior encountered and to test the predictions furnished by the relevant scenarios. In both of these potentials ϵ coincides with the negative of the contact value of the interaction, $\lim_{r\to\sigma+}(-w(r))$, and so sets the energy scale of the problem. The potential range is given by $1/z$ and $\lambda\sigma$, respectively. Unless stated otherwise, ϵ_0, the value of $w^{\text{hcy}}(r)$ inside the core, coincides with ϵ, a choice shared with the implementation by the authors of HRT and their coworkers referred to as the original one in refs. 9 and 10, q. v. A short summary of the parameter sets and sample isotherms considered in this study can be found in Table I. In the numerical work we employ an unconditionally stable implicit predictor-corrector scheme shortly characterized in Section 3.1. A more extensive discussion of the implementation can be found in refs. 9 and 10, where default settings for the most important customization parameters are also documented. Even further technical information is available with the source distribution itself.[11]

Of the three types of behavior compatible with the local properties of the PDE, both genuine ($r = s = 0$) and effective ($r > 0$, $s = r + 1 > 1$,

Table I. Overview of Systems and Sample Isotherms

System	$\beta_c\epsilon$	$\rho_c\sigma^3$	$\beta\epsilon$	$\rho_v\sigma^3$	$\rho_l\sigma^3$
SW, $\lambda = 3$	0.1011	0.26(1)	0.115	0.075(5)	0.510(5)
HCY, $z = 1.8/\sigma$	0.8316	0.33(1)	0.875	0.145(5)	0.525(5)

β_c and ρ_c give the location of the critical point, ρ_v and ρ_l the extent of the two-phase region at the inverse temperature β considered in the tables and figures to follow. The numbers have been obtained from HRT calculations not imposing the core condition. All of the digits indicated for β_c are significant.

$r_{\text{eff}} = s_{\text{eff}} = 0$) smoothness imply a FD approximation to f growing like $1/Q$. The monotonous scenario, on the other hand, furnishes the specific prediction that $\bar{\varepsilon}\, Q^2$ tends to a finite limit for $Q \to 0$. As we will see in Section 2, the numerical evidence clearly rules out this possibility.

It is thus only the genuinely smooth and the stiff scenarios that remain to be considered in Section 3. The results of the computations reported there do, indeed, allow us to infer the character of the PDE for subcritical temperatures, $T < T_c$, with great confidence, if only indirectly due to the great computational similarity of genuine and effective smoothness. Our main evidence in favor of the stiff scenario derives from the rather detailed and testable predictions it entails, all of which are confirmed numerically. By way of contrast, the genuinely smooth scenario does not hold an explanation for the observed trends, especially as regards the dependence of the FD results on the properties of the discretization grids.

Our conclusion that the PDE actually turns stiff in part of $\mathcal{D}$ for $T \leqslant T_c$ then paves the way for some heuristic arguments relating the onset of smoothing in Q to the form of the Fourier transform of the perturbational part of the potential (Section 4). So having understood the behavior of the PDE in the limit $Q \to 0$ where asymptotic reasoning valid for large $\bar{\varepsilon}$ applies, in Section 5 we then turn to similar computationally problematic features of its solution at much higher cutoff where the numerical evidence points to a mechanism not unlike that at work in the asymptotic region. We close with an informal discussion of the reasons for the atypical computational properties of HCY fluids of moderate inverse screening length z (Section 6).

2. THE MONOTONICITY ASSUMPTION REFUTED

According to Section V of part I[1], the assumption of a merely logarithmic divergence of f furnishes the rather specific prediction of $\bar{\varepsilon}\, Q^2$ tending to a finite limit for $Q \to 0$. Of course, the possibility of non-zero s means that, in principle, the smoothing effect discussed in Section VI of part I[1] must be reckoned with. The singularity being so mild, however, a possible reduction of $s > 0$ to an effective value of $s_{\text{eff}} = 0$ is preempted by the choice of step sizes ΔQ:

In our implementation of the theory the cutoff in the ith FD step is parameterized as

$$Q_{(i)} = \ln\left(e^{a - i\,b} + 1\right) \Big/ \sigma, \quad i = 0, 1, \ldots, \tag{4}$$

as is the case for the program the original authors of HRT and their coworkers employ, too. Here a/σ is close to the cutoff $Q_{(0)} \equiv Q_\infty$ where

initial conditions are imposed on f, and b/σ is the spacing $\Delta Q\big|_\infty$ of successive cutoffs in the large Q limit. For $Q \to 0$, on the other hand, we easily find $\Delta Q \approx -Q\left(1-e^{-b}\right)$. If $\bar{\varepsilon}\, Q^2$ is to approach zero or a finite constant as predicted by the assumption of monotonous growth these step sizes thus turn out of order $\mathbf{O}(\bar{\varepsilon}^{-1/2})$ at most, and our discretization should allow us to follow the variation of f reasonably well all the way to $Q=0$. From Fig. 1, however, we see that $\bar{\varepsilon}\, Q^2$ clearly diverges for $Q \to 0$. As this finding is corroborated by further calculations with a smaller setting of the numerical parameter $\Delta Q\big|_\infty$, on finer density grids (down to $\Delta\rho = 5 \cdot 10^{-4}/\sigma^3$), and for both hard-core Yukawa and square well potentials we feel we can safely exclude the monotonous growth scenario from further consideration.

3. SMOOTHNESS VERSUS STIFFNESS

As for the remaining two alternatives, an attempt to distinguish numerically between genuine and effective smoothness seems doomed at first sight: both predict a numerically smooth solution growing like $1/Q$ and with a profile like that sketched in Fig. 1 of part I[1]. And indeed, Fig. 2 shows the small Q behavior of f within the binodal as obtained numerically to be in excellent agreement with $f \propto 1/Q$, and Figs. 2, 3, and 5 as well as the numerical data demonstrate that f is of the form necessary for a stable pattern of growth, as postulated in part I[1], q. v. But even though these general features fit both scenarios, close scrutiny of the computational process and the numerical results yields a wealth of indirect evidence that we feel is sufficient to establish the stiffness of the

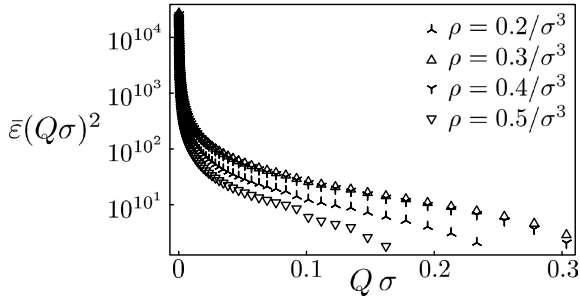

Fig. 1. $\bar{\varepsilon}\, Q^2$ as a function of Q for various densities inside the binodal. The data have been obtained for a hard-core Yukawa potential with inverse screening length $z = 1.8/\sigma$ and for an inverse temperature of $\beta = 0.875/\epsilon$. The numerical precision in the calculations was $\epsilon_\# = 10^{-2}$, the step size for infinite cutoff was $\Delta Q\big|_\infty = 10^{-2}/\sigma$.

PDE for $T < T_c$ with great confidence, if not with absolute certainty. We base our reasoning on the rather specific, and numerically testable predictions that follow from the assumption of stiffness. These stand in marked contrast to the vague expectations furnished by the genuinely smooth scenario that can, however, never be ruled out completely as smoothness is its sole defining characteristic. As we will show in this section, it is the assumption of a stiff PDE that is in full accordance with the numerical findings whereas smoothness is only marginally compatible with some of their traits, especially as regards the SW data.

Before, however, some general remarks are in place: Letting the labels x and y refer to either Q or ρ, in the stiff scenario smoothing in x sets in at $Q = Q_{\Delta x}$ and can always be postponed, i.e., shifted to lower cutoffs by decreasing the step size Δx. If, however, the corresponding exponent, r or s, is positive, the rapid growth of f, $\bar{\varepsilon}$ and $|\partial^2 f/\partial x^2|$ as the solution proceeds towards $Q = 0$ implies that the amount by which $Q_{\Delta x}$ can be changed in this way and the attendant computational effects must be small. For positive exponents the $Q_{\Delta x}$ are thus fairly well defined despite the gradual nature of the transition to the smoothing regime. – Furthermore, without loss of generality assuming $Q_{\Delta x} > Q_{\Delta y}$, $Q_{\Delta x}$ is obviously independent of the step sizes Δy. The solution obtained numerically at cutoffs below $Q_{\text{smooth}} \equiv Q_{\Delta x}$ is already affected by smoothing in x so that there is no point in identifying $Q_{\Delta y}$ with the cutoff where Δy becomes too large to describe the variation of the no longer accessible true solution of the PDE. Instead, $Q_{\Delta y}$ is taken to be the cutoff where smoothing in y commences in the solution of the FD equations (FDEs), which implies a Δx dependence of $Q_{\Delta y}$ and may even induce $Q_{\Delta y}$ to vanish altogether. For $Q < Q_{\Delta y}$, the solution generated numerically by necessity conforms to the smooth scenario as $r_{\text{eff}} = s_{\text{eff}} = 0$ and so grows like $1/Q$ in a stable manner. This proportionality also means that the form of f remains constant from $Q_{\Delta y}$ all the way to the final results at zero cutoff. (Here and below the form of f at some cutoff Q refers to $f(Q, \rho)$ as a function of ρ, restricted to $\rho_1 < \rho < \rho_2$ and without regard for the overall normalization of f.) – The important mechanism sketched in Section III of part I[1] and the concomitant stabilization of form and monotonicity of f do not explicitly depend on s and thus always set in at $Q_{\Delta\rho}$; incidentally, Figs. 2 and 3 show its preconditions, viz., flatness and compatibility with the sketch of part I[1] to be met numerically. Of course, both $Q_{\Delta Q}$ and $Q_{\Delta\rho}$ depend on temperature and density, which is taken to be silently accounted for whenever we speak of the form of f at one of the $Q_{\Delta x}$, and they are defined only in that part of $\mathcal{D}$ where f is large. – Not surprisingly, the two possible orderings for the cutoffs $Q_{\Delta Q}$ and $Q_{\Delta\rho}$ assigned in an interpretation of the numerical results in terms of the stiff scenario

entail vastly different consequences and are therefore discussed separately in subsections 3.2 ($Q_{\Delta\rho} > Q_{\Delta Q}$) and 3.3 ($Q_{\Delta Q} > Q_{\Delta\rho}$) below.

Before that, however, it is worthwhile to step back for a moment and ask why we have to adopt Eq. (1) in the first place if the most direct formulation of the theory is that of a PDE for the free energy $A^{(Q)}(\rho)$ of the Q system at density ρ, cf. part I[1]. Indeed, from Eqs. (A2) and (A3) of part I[1] we see that $\partial A^{(Q)}/\partial Q \propto Q^2 (f + \text{const})$ for $Q\sigma \ll 1$ so that the Q and ρ scales characteristic of $A^{(Q)}(\rho)$ are essentially the same as for $f(Q, \rho)$. In the smooth scenario there is then no reason for the formulation in terms of f to be preferable to that in terms of the free energy, provided proper care is taken to ensure stability and convergence. This has certainly been the case in our earlier work shortly summarized in appendix B.1 of ref. 10 that nevertheless was unable to proceed to small Q for $T < T_c$. Similar difficulties are reported in ref. 6, and to the best of our knowledge there are no HRT results on simple one-component fluids for $T < T_c$ except in the quasilinear formulation of Eq. (1) or variants thereof. – In the stiff scenario all this is, of course, to be expected as the rapid low amplitude oscillations of the solution in this case necessitate step sizes that are reduced as some inverse power of $\bar{\varepsilon}$ or the exponential of $\partial A^{(Q)}/\partial Q$, and only under special circumstances do the discretized equations allow one to obtain a solution with the much larger step sizes used in practical applications. As noted in Section II of part I[1], the auxiliary quantity $f(Q, \rho)$ was introduced exactly for this reason.[8]

3.1. Numerical Aspects

As some of the numerical effects are rather subtle, we should also recall several key aspects of the implementation we rely on. This is a highly flexible and fully modular computational framework for the solution of a FD approximation of the PDE by an implicit predictor-corrector scheme thoroughly discussed in refs. 9 and 10. For consistency with part I,[1] in the calculations reported here we refrain from implementing the core condition. The discretization is applied on uniform density grids and with the predetermined step sizes ΔQ of Section 2. Convergence of the FD equations has been checked, and iteration of the corrector step does not bring about noticeable changes.

In practical applications, the discretized equations generally cannot be solved down to arbitrarily small Q for $T < T_c$, and the smallest cutoff reached we denote $Q_{\min}$. As the failure modes responsible for an end of the program are known[9,10] and can be linked to the local behavior of the solution, *v. i.*, the systematic changes in $Q_{\min}$ upon variation of aspects of the numerical procedure provide a powerful and readily accessible

diagnostic tool. For the calculations reported here, the immediate cause for abortion of the computation at some cutoff $Q_{\min}$ is either an insufficient adaptation of the rescaling necessary for representing quantities affected by exponentiation of f – the scale of Fig. 1 alone shows that, e.g., $\bar{\varepsilon}$ cannot be represented in double precision – or else because of non-real f and negative $\varepsilon \equiv \bar{\varepsilon} + 1$ in the predictor step. These two effects are linked to rapid increase and decrease of f, respectively.

Unlike the $Q_{\Delta x}$, $Q_{\min}$ obviously does not depend on the density. Instead, it is essentially determined by the physical potential $w(r)$, the temperature, the discretization grid, and the formulation of the theory.[9] As for the latter, if the PDE is coupled to further constraints, and the solution vector augmented by additional components to be determined accordingly, the likelihood of an early termination of the computation in the predictor step generally increases, and so does $Q_{\min}$. As the customary manner of implementing the core condition involves an expansion of the direct correlation function inside the core,[6,9] the sensitivity of $Q_{\min}$ to an increase in N_{cc}, the number of expansion coefficients, again proves of interest.

For a more detailed account we refer the reader to refs. 9 and 10 as well as the documentation that comes with the source code distribution itself.[11]

3.2. Smoothing in ρ First

So let us first turn to the HCY fluid of inverse screening length $z = 1.8/\sigma$ already considered in ref. 9. As mentioned before, the numerical solution must be smooth at any rate and is therefore always compatible with the genuinely smooth scenario. In this case, we expect only a small dependence of the results on ΔQ and $\Delta\rho$ that should be essentially stochastic in nature, stemming from the truncation error in an otherwise unproblematic FD approximation of the PDE alone.

As we shall see in a moment, the numerics can also be reconciled with the stiff scenario if only we assume smoothing to occur in the ρ direction first, $Q_{\Delta\rho} > Q_{\Delta Q}$, furnishing the following predictions: The mechanism responsible for stable growth of f (cf. Section III of part I[1]) being at work at all cutoffs below Q_{smooth}, the stability of the computational process is not an issue and incorporation of the core condition is entirely unproblematic. An overflow due to an insufficient adaptation of the rescaling of non-$\mathbf{O}(1)$ quantities is the only possibility for numerical failure, and its likelihood is greatly reduced when ΔQ is decreased so that smaller step sizes are generally accompanied by smaller values of $Q_{\min}$. A systematic $\Delta\rho$ dependence of $Q_{\min}$ is not anticipated. – For fixed density grid,

$Q_{\Delta\rho} \equiv Q_{\text{smooth}}$ cannot depend on ΔQ, nor can f at $Q_{\Delta\rho}$. On the other hand, even though smaller step sizes, i. e., smaller $\Delta Q\big|_{\infty}$, cf. Section 2, correspond to smaller $Q_{\Delta Q}$, $s > 1$ implies that the drop in $Q_{\Delta Q}$ must be exceedingly small. As furthermore the evolution from $Q_{\Delta\rho}$ down to $Q_{\Delta Q}$ is determined by the solution at the onset of smoothing and the properties of only the density grid, the form of f below $Q_{\Delta Q}$, including $Q = 0$, is virtually ΔQ independent. – As for a variation of the density grid at fixed ΔQ, a reduction of $\Delta\rho$ clearly entails a shift of $Q_{\text{smooth}} \equiv Q_{\Delta\rho}$ to smaller cutoffs, which may in turn cause a change in $Q_{\Delta Q}$, too. These effects must be rather small because of the non-zero exponents r and s, and they must vary with the density for the same reason the $Q_{\Delta x}$ are density dependent. A change of the ρ grid thus implies a small change of the form of f at $Q_{\Delta\rho}$ and, hence, at $Q_{\Delta Q}$ and all smaller cutoffs. As long as $Q_{\Delta\rho}$ does not fall below $Q_{\Delta Q}$, however, the ratio of the forms of f as obtained on different density grids cannot depend on ΔQ.

All these predictions are confirmed in the actual calculations for a HCY potential with $z = 1.8/\sigma$ on density grids with $\Delta\rho = 10^{-2}/\sigma^3$ and $\Delta\rho = 5 \cdot 10^{-4}/\sigma^3$ and varying ΔQ as summarized in Tables II–IV and Fig. 2. For fixed density grid (Tables II and III, respectively), $Q_{\min}$ and, hence, the final values of f markedly depend on ΔQ, the former generally decreasing and the latter increasing upon reduction of the step size. On the other hand, both the form of f and its magnitude at fixed cutoff – to be found in the tables under the headings of F_x^y and $f_x\, Q_{\min}\sigma$, respectively – remain largely unchanged. Comparing the results obtained with differ-

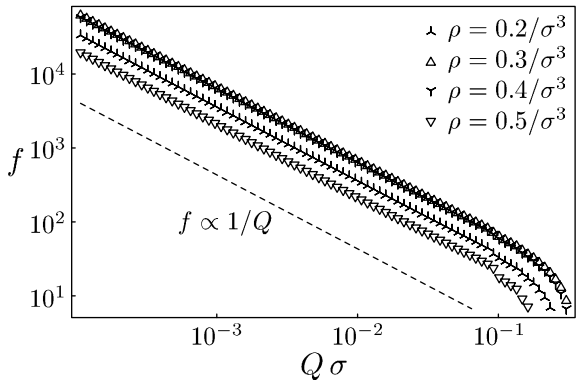

Fig. 2. f as a function of Q for various densities inside the binodal. The data have been obtained for the same hard-core Yukawa potential and with the same numerical parameters as in Fig. 1. The dashed line indicates the slope corresponding to proportionality of f to the reciprocal of the cutoff. Subsequent symbols are separated by 10 steps in the $-Q$ direction.

ent settings for $\Delta\rho$, the change in the final values of f is indeed almost completely due to the differences in $Q_{\min}$. The magnitude at fixed Q, on the other hand, is affected only moderately, viz., by a few per cent for a 20-fold increase in the density resolution, and it depends on ρ but not on ΔQ, cf. Table IV. $Q_{\min}$ itself is not affected by the density grid in a systematic way. There are two sample isotherms, viz., the ones at $\Delta Q\big|_\infty = 0.003/\sigma^3$, $\Delta\rho = 10^{-2}/\sigma^3$ and at $\Delta Q\big|_\infty = 0.004/\sigma^3$, $\Delta\rho = 5\cdot 10^{-4}/\sigma^3$, that founder at comparatively large cutoff. Of these, only the former does not enter the asymptotic regime where $f \propto 1/Q$, as can clearly be seen from Table IV. All in all, the numerical results are in excellent agreement with stiffness, and we note that for this system and the density grids considered $Q_{\Delta Q}$ must be sought around $10^{-2}/\sigma$. Trivially, being smooth the results also conform to the smooth scenario as mentioned before.

3.3. Smoothing in *Q* First

In our previous work on HRT[9,12] we repeatedly stressed the vastly different numerical properties of the HCY and SW potentials. This is certainly not anticipated for genuine smoothness that merely predicts a

Table II. ΔQ Dependence of the Final Results for a Hard-Core Yukawa System

$\Delta Q\big\|_\infty \sigma$	$Q_{\min}\sigma$	$f_{0.2}$	$f_{0.2}\,Q_{\min}\sigma$	$F_{0.2}^{0.3}$	$F_{0.2}^{0.4}$	$F_{0.2}^{0.5}$
0.003	$9.914\cdot 10^{-3}$	$3.643\cdot 10^{2}$	3.612	1.862	1.755	0.590
0.004	$3.995\cdot 10^{-5}$	$8.990\cdot 10^{4}$	3.592	1.867	1.758	0.585
0.005	$5.014\cdot 10^{-5}$	$7.163\cdot 10^{4}$	3.592	1.867	1.758	0.585
0.010	$9.943\cdot 10^{-5}$	$3.612\cdot 10^{4}$	3.592	1.867	1.758	0.585

Just as in Figs. 1 and 2, $z = 1.8/\sigma$, $\beta = 0.875/\epsilon$, and $\Delta\rho = 10^{-2}/\sigma^3$. We use the notation f_x for $f(Q_{\min}, x/\sigma^3)$ and define $F_x^y \equiv f_y/f_x$.

Table III. ΔQ Dependence of the Final Results for a Hard-Core Yukawa System

$\Delta Q\big\|_\infty \sigma$	$Q_{\min}\sigma$	$f_{0.2}$	$f_{0.2}\,Q_{\min}\sigma$	$F_{0.2}^{0.3}$	$F_{0.2}^{0.4}$	$F_{0.2}^{0.5}$
0.003	$3.131\cdot 10^{-5}$	$1.167\cdot 10^{5}$	3.652	1.865	1.768	0.625
0.004	$1.004\cdot 10^{-2}$	$3.638\cdot 10^{2}$	3.653	1.865	1.768	0.625
0.005	$5.014\cdot 10^{-5}$	$7.285\cdot 10^{4}$	3.652	1.865	1.768	0.625
0.010	$1.004\cdot 10^{-4}$	$3.637\cdot 10^{4}$	3.653	1.865	1.768	0.625

The parameters and notation coincide with those of Table II, except for $\Delta\rho = 5\cdot 10^{-4}/\sigma^3$.

Table IV. $\Delta\rho$ Dependence of the Form of the Final Results for a Hard-Core Yukawa System at Varying ΔQ

$\Delta Q\big\vert_\infty \sigma$	$G_{0.2}$	$G_{0.3}$	$G_{0.4}$	$G_{0.5}$
0.003	1.011	1.013	1.018	1.072
0.004	1.017	1.016	1.022	1.087
0.005	1.017	1.016	1.022	1.086
0.010	1.017	1.016	1.022	1.086

The parameters coincide with those of Table II and III. Perusing the notation introduced there, G_x is $f_x\, Q_{\min}\sigma$ as evaluated for $\Delta\rho = 5 \cdot 10^{-4}/\sigma^3$ divided by the same quantity for $\Delta\rho = 10^{-2}/\sigma^3$.

small grid dependence stemming from the local truncation error of the discretization, exactly as for the HCY system. Still, the assumption of a genuinely smooth solution is certainly compatible with the numerics, if only marginally so in the face of the most prominent feature of the evolution of f, viz., episodes of much more rapid variation than mere proportionality to $1/Q$.

Assuming the PDE to turn stiff for large f instead, and furthermore $Q_{\Delta Q}$ to exceed $Q_{\Delta\rho}$ for the present system, there is a Q range $Q_{\Delta\rho} < Q < Q_{\Delta Q}$ where FDEs are used with inappropriately large step sizes ΔQ while oscillations in ρ are not yet suppressed. For these cutoffs, the stabilization wrought by the mechanism analyzed in Section III of part I[1] is not effective yet, and there is no reason for f to be convex from below throughout the density range $\rho_1 < \rho < \rho_2$. On the other hand, the overall profile of f is expected to resemble Fig. 1 of part I[1], and $s_{\text{eff}} = 0$ once more suggests a general growth proportional to $1/Q$. The sign of $\partial^2 f/\partial\rho^2$ is thus unconstrained, and its modulus increases in unison with f, i.e., in proportion to $1/Q$. As d_{00}/d_{02} is of order $\mathbf{O}(1)$, however, the $\mathbf{O}(1)$ growth of $\partial^2 f/\partial\rho^2$ may well be sufficient to destabilize the growth at some $Q \in (Q_{\Delta\rho}, Q_{\Delta Q})$, prompting much more rapid variation of f as a function of Q. Of course, these near-discontinuities of f will occur at different cutoffs for different densities, most often close to ρ_1 and ρ_2 where the $Q_{\Delta x}$ are smallest, and neighboring densities will experience them at roughly the same cutoff. Furthermore, in principle the jumps should lead to both increases and decreases in f, depending on the sign of $\partial^2 f/\partial\rho^2$ at slightly larger Q. Considering the numerics, however, a large change in f is almost certain to bring the calculation to an end, and all the failure modes discussed in Section 3.1 are relevant for $Q_{\min}$. A comparatively mild increase of f, on the other hand, may relax the relative curvature of f to the point of allowing the solution to enter once more an episode of near-stability characterized by growth in approximate proportion

to $1/Q$. As for an incorporation of the core condition, in accordance with Section 3.1 the attendant introduction of additional degrees of freedom is likely to exacerbate the risk of triggering such a jump in f, cf. Section 5. – To understand the grid dependence of the numerics under the assumption of stiffness, recall that $Q_{\min}$ itself is the location of a failed jump in f. As smoothing in Q is the driving force behind the computational process, $Q_{\min}$ must be quite sensitive to ΔQ, but there is no reason for $Q_{\min}$ to be monotonous in ΔQ. The density grid, on the other hand, is still adequate for the elliptic boundary value problem in ρ at constant Q. If the numerical process were stable, there should thus be no appreciable dependence of the results on $\Delta\rho$ at all. In the absence of the stabilization wrought by smoothing in ρ, however, even the small differences seen upon variation of $\Delta\rho$ must be expected to shift the episodes of rapid evolution to slightly different cutoffs in an unsystematic way. By the same token, the $\Delta\rho$ dependence of the final form of f should be small, and different ΔQ should leave it unaltered as long as the number and the approximate positions of the jumps do not change. As those are least frequent close to the maximum of f, its form is expected to be most stable in the central part of the density interval of large f.

Again, these predictions compare favorably with the numerical results for a SW potential of range $\lambda = 3$ obtained on the same discretization grids as the HCY data of Section 3.2. The most prominent feature, barely compatible with genuine smoothness, viz., near-discontinuities of f can actually be found in the numerical data underlying Tables V and VI at the locations marked with arrows in Fig. 3; indeed, several of them can be

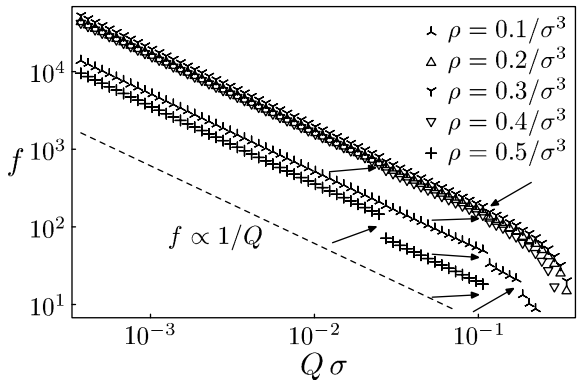

Fig. 3. f as a function of Q for various densities inside the binodal. The data have been obtained for a SW potential with $\lambda = 3$ and at a temperature of $\beta = 0.115/\epsilon$; otherwise, the remarks of Fig. 2 apply. Arrows mark several of the near-discontinuities discussed in Section 3.3.

Table V. ΔQ Dependence of the Final Results for a SW System

$\Delta Q\big\vert_\infty \sigma$	$Q_{\min}\sigma$	$f_{0.15}$	$F_{0.15}^{0.25}$	$F_{0.25}^{0.35}$	$F_{0.35}^{0.45}$
0.003	$4.181\cdot 10^{-4}$	$-1.415\cdot 10^{5}$	2.379	1.635	0.392
0.004	$3.198\cdot 10^{-4}$	$3.597\cdot 10^{4}$	1.589	0.965	0.523
0.005	$3.318\cdot 10^{-4}$	$3.465\cdot 10^{4}$	1.589	0.965	0.523
0.010	$3.576\cdot 10^{-4}$	$3.225\cdot 10^{4}$	1.589	0.965	0.523

Just as in Fig. 3 $\lambda=3$, $\beta=0.115/\epsilon$, and $\Delta\rho=10^{-2}/\sigma^3$. The Notation is the Same as in Table II.

seen clearly even on the logarithmic scale of the graph. All the other consequences of stiffness with $Q_{\Delta Q} > Q_{\Delta\rho}$ are also in agreement with the data of Tables V and VI: In particular, a pronounced ΔQ dependence of $Q_{\min}$ is accompanied by only a very modest effect as $\Delta\rho$ is varied, even though the relative change in $\Delta\rho$ is much larger than that in ΔQ. Excluding the pathological data with negative f (*v. i.*), the final forms of f are mostly ΔQ independent, and the forms obtained on the two density grids differ but slightly. Only the isotherm with $\Delta Q\big\vert_\infty = 0.010/\sigma$ in Tab. VI presents a somewhat different shape than those at smaller $\Delta Q\big\vert_\infty$. The differences in the numbers given under the heading F_x^y are, however, still in accordance with the stiff scenario as discrepancies appear only close to the edge of the density range of large f. As for the first entry of Table V ($\Delta Q\big\vert_\infty = 0.003/\sigma$), negative f corresponds to exceedingly small values of $\varepsilon \equiv \bar{\varepsilon} + 1 \sim 10^{-27}$. This is found to be the result of a downward jump from $f \sim +10^4$ ($\varepsilon \sim 10^{5000}$) at only slightly higher cutoff where the form of f again corresponds to that of the other isotherms. Clearly, even a minor perturbation of the numerical process might easily have led to negative ε and hence to a numerical exception; in this case our implementation would have discarded the last step, and the final results would once more conform with those of the remainder of Table V.

Let us shortly return once more to the most salient feature of the numerical solution, viz., its near-discontinuities. Disregarding the analytical considerations of part I[(1)] it might be tempting to imagine that, for $T < T_c$, the PDE generates a shock front approximately symmetrically moving outward towards the densities ρ_v and ρ_l of the coexisting phases as Q approaches zero. In this view of the numerical process the jumps occur when the shock reaches the corresponding density. Such an interpretation is not consistent with the data. According to Fig. 3, the near-discontinuities of f occur repeatedly at the same density (most conspicuously for $\rho = 0.1/\sigma^3$), and rapid change at one density is generally

Table VI. ΔQ Dependence of the Final Results for a SW System

$\Delta Q\|_\infty \sigma$	$Q_{\min}\sigma$	$f_{0.15}$	$F_{0.15}^{0.25}$	$F_{0.25}^{0.35}$	$F_{0.35}^{0.45}$
0.003	$4.206 \cdot 10^{-4}$	$2.812 \cdot 10^{4}$	1.584	0.974	0.547
0.004	$3.302 \cdot 10^{-4}$	$3.589 \cdot 10^{4}$	1.584	0.974	0.547
0.005	$3.318 \cdot 10^{-4}$	$3.551 \cdot 10^{4}$	1.584	0.974	0.547
0.010	$3.685 \cdot 10^{-4}$	$3.178 \cdot 10^{4}$	1.589	0.974	0.545

The parameters and notation coincide with those of Table V, except for $\Delta\rho = 5 \cdot 10^{-4}/\sigma^3$.

accompanied by similar behavior at other densities. Neither of these observations is compatible with the idea of a moving shock front, nor is there any reason why the binodal should be linked to a shock front in SWs but not in the HCY fluid, cf. Section 3.2.

3.4. Assertion of Stiffness

Summarizing the numerical evidence presented so far we find that of the three scenarios found in part I[1] only the possibility of a merely logarithmic singularity of f can be ruled out with certainty. We are then faced with the two alternatives of genuine smoothness of the PDE on the one hand, and effective smoothness as a result of an FD approximation to a stiff PDE on the other hand. As shown in the preceding subsections 3.2 and 3.3, neither of them is in direct contradiction with the numerical data.

The crucial difference is their respective specificity and testability: The genuinely smooth scenario does not make any predictions beyond the smallness of the discretization grid dependence of the numerical results, nor does it offer any of the detailed understanding of the computational process that is necessary for accurate and reliable interpretation of the FD results. By way of contrast, stiffness of the PDE in part of its domain provides a consistent framework for the interpretation of the numerics and furthermore entails a number of concrete and numerically testable consequences, all of which are in excellent agreement with our data once the correct ordering of the $Q_{\Delta x}$ has been chosen. In combination with the analytical considerations of part I[1] and our earlier statements regarding the importance of the formulation of the HRT PDE employed, the specificity and great number of these predictions provide ample, although necessarily indirect evidence in favor of the stiff scenario.

From this point on we will therefore take it for granted that the HRT PDE does, indeed, turn stiff in part of its domain for subcritical

temperatures. On this basis, we now aim to further enhance our understanding of the HRT numerics, shedding some light on the location of $Q_{\Delta Q}$ (Section 4), extending our findings in the asymptotic region to intermediate Q (Section 5), and finally clarifying the outstanding numerical properties of the HCY potential *vis-à-vis* other physical systems (Section 6).

4. THE ONSET OF SMOOTHING IN Q

Considering the great importance of the relative order of the $Q_{\Delta x}$ for the numerical process, it is natural to inquire into their typical values. As the exponents r and s are non-zero by assumption, these cutoffs may only weakly depend on the discretization grid and so are largely determined by the perturbational part of the potential alone. Whereas the onset of smoothing in ρ eludes simple reasoning so far, some heuristic arguments point to a simple connection between the likelihood of finding $Q_{\Delta Q}$ at some cutoff and the form of the Fourier transform $\tilde{w}(k)$.

Let us consider a thermodynamic state of diverging isothermal compressibility at a cutoff that is low enough for smoothing in Q to have set in at least partially, $Q \sim Q_{\Delta Q}$. In view of the gradual transition between the smoothing and non-smoothing regimes, the effective exponent s_{eff} may not vanish exactly yet; nevertheless it seems safe to assume $s_{\text{eff}} < 1$. Of course we expect $\bar{\varepsilon} \gg f \gg 1$ so that reasoning based on the asymptotic behavior for large $\bar{\varepsilon}$ is applicable, and due to the monotonicity of the exponential function the likelihood of finding $Q_{\Delta Q}$ close to some cutoff Q increases with the slope $-\partial f/\partial Q$ of f. At the same time, for a hard-sphere reference system $Q_{\Delta Q}$ can only depend on the form of the Fourier transform of the perturbational part of the interaction potential, i.e., on $\tilde{u}_0 = \tilde{\phi}/\tilde{\phi}_0$ rather than on $\tilde{\phi}$ itself. The temperature $T = 1/k_B\beta$ enters the calculation only as a pre-factor to the interaction potential, viz., through $\phi = -\beta w$ so that the normalization of $\tilde{\phi}$ only fixes an energy or temperature scale.

With this in mind we define an auxiliary quantity $\psi(Q, \rho)$, corresponding to $\tilde{\phi}_0 + \gamma_0^{(Q)}$ in the notation of our earlier work on HRT,[1,9,10,12] through

$$\tilde{K} + \psi\,\tilde{u}_0 = -\frac{\tilde{\phi}}{\bar{\varepsilon}}. \tag{5}$$

Solving this relation for ψ and differentiating with respect to Q we obtain

$$\frac{\partial \psi}{\partial Q} = -\tilde{\phi}_0 \left(\frac{\partial}{\partial Q}\frac{1}{\bar{\varepsilon}} + \frac{\partial}{\partial Q}\frac{\tilde{K}}{\tilde{\phi}} \right), \tag{6}$$

which is valid at all cutoffs except close to the zeros $Q_{\tilde{\phi},i}$ of $\tilde{\phi}$ and $\tilde{u}_0$ where Eq. (5) cannot be inverted. – An alternative expression for $\partial\psi/\partial Q$ can be obtained from the PDE (1) and the compressibility sum rule. Following Section 2.4.1 of ref. 10, for density independent potential we easily find

$$\begin{aligned}\frac{\partial\psi}{\partial Q} &= -\frac{Q^2}{4\pi^2}\frac{\partial^2}{\partial\rho^2}\ln\varepsilon \\ &= \frac{Q^2}{4\pi^2}\left(-\tilde{u}_0^2\frac{\partial^2 f}{\partial\rho^2}+\tilde{\phi}\frac{\partial^2}{\partial\rho^2}\frac{1}{\tilde{\mathcal{K}}}\right).\end{aligned} \tag{7}$$

Equating these two expressions for $\partial\psi/\partial Q$, solving for $\partial^2 f/\partial\rho^2$, and inserting the result into the PDE (1) yields

$$\frac{\partial f}{\partial Q} = d_{00}+\frac{d_{02}\,4\pi^2}{Q^2\,\tilde{u}_0^2}\left(\tilde{\phi}_0\frac{\partial}{\partial Q}\frac{1}{\bar{\varepsilon}}+\frac{\partial}{\partial Q}\frac{\tilde{\mathcal{K}}}{\tilde{u}_0}\right)+\frac{d_{02}\,\tilde{\phi}_0}{\tilde{u}_0}\frac{\partial^2}{\partial\rho^2}\frac{1}{\tilde{\mathcal{K}}} \tag{8}$$

for Q away from the $Q_{\tilde{\phi},i}$. Both d_{00} and d_{02} are negative in the case under consideration.[1]

Of the expressions appearing on the right hand side of Eq. (8) the one involving the Q derivative of $1/\bar{\varepsilon}$ is of order $\mathbf{O}(\bar{\varepsilon}^{s_{\text{eff}}-1})$ and so can be neglected if $s_{\text{eff}}<1$ as assumed. As we are looking for an effect triggered by the form of $\tilde{\phi}$ alone we do not have to consider the derivatives of the properties of the hard sphere reference system encoded in $\tilde{\mathcal{K}}$ either. It is then the term involving the Q derivative of $\tilde{u}_0$ that is of interest. The ideal gas contribution $-1/\rho$ to $\tilde{\mathcal{K}}$ ensures positive $d_{02}\tilde{\mathcal{K}}$ so that this term is the product of $\partial\tilde{u}_0/\partial Q$ and manifestly positive factors. Now assume that $Q_{\Delta Q}$ is less than the position of the first minimum of $\tilde{u}_0$ so that only the monotonous growth of $\tilde{u}_0$ towards its global maximum at $Q=0$ remains to be covered by the solution of the PDE. Clearly, as the calculation proceeds in the negative Q direction, the steeper this rise of $\tilde{u}_0$, the more the $\partial\tilde{u}_0/\partial Q$ term counteracts the growth of f, thereby effectively further delaying the onset of smoothing in Q. Most likely, $Q_{\Delta Q}$ will thus be found at cutoffs so low that $\tilde{u}_0$ already levels off towards its limiting value of unity.

For the two potentials considered earlier, viz., SWs and the HCY system with $z=1.8/\sigma$, Fig. 4 shows that $\tilde{u}_0$ levels off when Q (or λQ, in the case of SWs) is no more than about $10^{-1}/\sigma$, which is well compatible with the estimate of Section 3.2. In addition, Figs. 2 and 3 demonstrate that

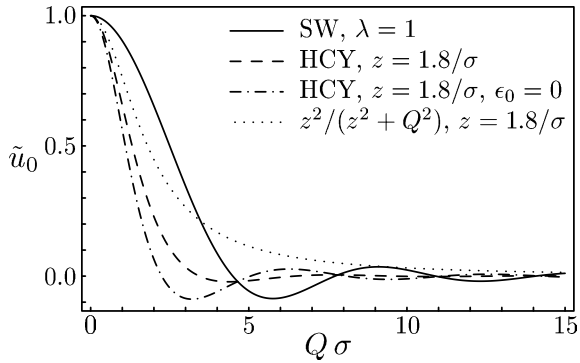

Fig. 4. $\tilde{u}_0$ as a function of Q for SW and HCY potentials with the parameters indicated. If, contrary to Eq. (2), the Yukawa form is retained even inside the core, $\tilde{u}_0(Q)$ is given by $z^2/(z^2 + Q^2)$. As far as the SW potential is concerned, λ and Q enter $\tilde{u}_0$ only in the combination λQ so that a variation of the potential range only introduces a linear rescaling of the Q dependence of the function. We have checked that the graph remains qualitatively unchanged for different parameter settings. The first minimum of $\tilde{u}_0$ is -0.02 for the default HCY potential, -0.09 for the HCY potential with $\epsilon_0 = 0$, and slightly above -0.09 for the SW potential.

the transition to the regime where f mostly grows like $1/Q$, corresponding to vanishing s_{eff}, occurs at similar values of the cutoff. All in all, our arguments, heuristic as they are, do indeed allow us to estimate $Q_{\Delta Q}$ in a satisfactory way. As for smoothing in ρ, on the other hand, actual numerical solution of the PDE currently is the only way of locating and studying $Q_{\Delta\rho}(T, \rho)$.

5. BEYOND ASYMPTOTICS

On the basis of the results presented so far one might expect numerical difficulties to first surface close to $Q_{\Delta x}$, i.e., around $Q \sim 10^{-1}/\sigma$ for the potentials considered earlier. However, the monitoring variant of our code[9–11] that must be credited with first highlighting the stiffness of the equations clearly signals the inadequacy of the discretization grid already at much higher cutoff, viz., typically for $5 < Q\sigma < 10$. Indeed, the asymptotic region of large $\bar{\varepsilon}$ can never even be reached without renouncing control of the local truncation error in solving the FDEs, cf. Section III E of ref. 9.

In combination with the observed patterns of the evolution of f at intermediate and small Q illustrated in Figs. 2, 3 and 5, our experience with the numerics of HRT leads us to propose that stiffness is not

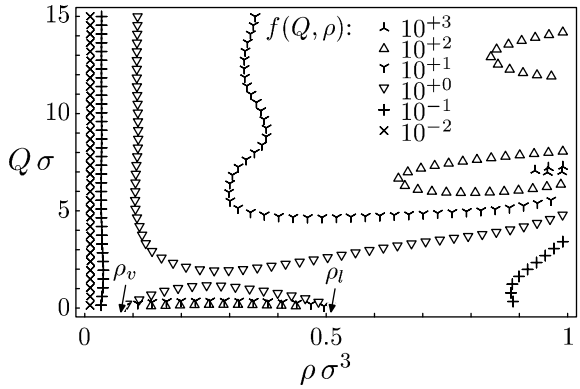

Fig. 5. $f(Q,\rho)$ for intermediate cutoff as a logarithmic contour plot. The data has been obtained for SWs with $\lambda=3$ at inverse temperature $\beta=1/k_B\,T=0.115/\epsilon$. Both the approach to the low-density boundary condition of vanishing f at densities below $0.01/\sigma^3$ and the final build-up of infinite compressibility at cutoffs below $10^{-1}/\sigma$ have been excluded from the graph.

confined to that part of $\mathcal{D}$ where the final build-up of infinite κ_T takes place. Indeed, Fig. 5 shows that there are several regions of large f at higher cutoff, some of which may give rise to transient stiffness of the PDE. Even though the analysis of part $\mathrm{I}^{(1)}$ does not apply directly – f being bounded, asymptotic reasoning is not guaranteed to be valid, nor does large f imply large $\bar{\varepsilon}$ any longer due to the smallness of $\tilde{u}_0^2$ –, from the expressions given in part $\mathrm{I}^{(1)}$ we can still deduce that d_{02} is negative and appreciable for all Q in the relevant cutoff range except very close to the $Q_{\check{\phi},i}$, and that d_{00} is likely to be rather large in modulus for $f\gg 1$ due to the terms linear in f. Depending on the sign of d_{00}, large f may well prompt rapid further growth when Q proceeds to smaller values. Just as in Section 3.3, such a rapid growth of f almost certainly induces an accompanying growth of $|\partial^2 f/\partial\rho^2|$ on the grid, and any oscillations of the density curvature will carry over to $\partial f/\partial Q$. Qualitatively the situation is then quite similar to that in the asymptotic region, and it seems reasonable to see this transient stiffness at intermediate cutoff as preventing computations insisting on local convergence on a dynamically adjusted discretization mesh to ever proceed to $Q\sim Q_{\Delta x}$.

Without the backing of more formal arguments much of the above line of thought may seem insubstantial. There are, however, a number of numerical effects that provide at least indirect evidence for the point of view just laid out. Among those already discussed in our earlier work on HRT, the plummeting step sizes observed when determining the discretization grid from the local curvature of appropriate components of

the solution vector[9,11] are the most direct sign of stiffness at intermediate Q. Further support comes from our study of SWs of varying range.[12] There the peculiar shifts in the critical temperature whenever λ is close to a simple fraction have been linked to the modulation of $\bar{\varepsilon}$ by the interference of $\tilde{c}_2^{\mathrm{ref}}$ and $\tilde{\phi}$; and considering our remarks on the effect of extending the solution vector (Section 3.1) it is significant that the critical point is accessible in a wider λ range when coupling the PDE to a smaller number of expansion terms for taking into account the core condition, cf. Section IV E of ref. 12 and appendix E of ref. 10. Transient stiffness also explains why the lowest temperature attainable numerically, denoted $1/k_B\beta_{\max,\#}$ in refs. 10 and 12, may well be higher than T_c even though stiffness in the asymptotic region is a problem only for $T \leqslant T_c$, and that the isotherms show no sign of phase separation for $\beta < \beta_{\max,\#} < \beta_c$, the critical temperature being known independently from related computations or by other methods. – There are also some more intricate issues related to the interplay of the $Q_{\tilde{\phi},i}$ (where d_{00} vanishes as $\tilde{\phi}^2$) with the boundaries of the cutoff ranges where the step sizes ΔQ are inappropriate, as well as to the ρ dependence of the onset of smoothing in the presence of a local density grid refinement. Discussion of these subtle effects and their numerical manifestations requires a detailed presentation of appropriate methods of data analysis on non-uniform high-resolution density grids and so falls outside the scope of the present report.

6. HARD-CORE YUKAWA VERSUS OTHER POTENTIALS

In conjunction with our earlier analyses of the issues surrounding initial and high density boundary conditions, implementation of the core condition, and the peculiarities of discontinuous potentials,[9,10,12] assertion of stiffness at low and intermediate Q below a certain temperature provides us with a detailed understanding of the numerical process of solving the HRT PDE throughout $\mathcal{D}$ and has proved invaluable in interpreting numerical raw data. We close this short series of reports with a generally relevant sample of the kind of insight that can be gained on this basis, viz., a clarification of the unusually benign computational properties of the HCY potential.

Throughout our numerical work we consistently found that HCY fluids of moderate inverse screening length like, e. g., the one with $z = 1.8/\sigma$ repeatedly used here and in ref. 9 exhibit the symptoms of stiffness only in a rather mild form, both for $Q \to 0$ where this follows from the low value of $Q_{\Delta Q}$, and at intermediate cutoff. This can be understood by noting, firstly, that the temperature enters the calculation only through $\tilde{\phi} = -\beta w$, the global normalization of which is accessible only in the limit

$Q \to 0$. At any cutoff Q, the variation of $\tilde{\phi}(k)$ for $k > Q$ is then the only measure of the temperature available to the PDE; at the same time, for every one of the patches of large f, stiffness arises only below some characteristic temperature, coinciding with the critical one for the final build-up of infinite κ_T at $Q = 0$. Secondly, recalling that $\tilde{u}_0 \propto \tilde{\phi}$, a look at Fig. 4 and the numbers quoted in its caption shows that the local extrema at $Q > 0$ of $\tilde{\phi}^{\text{hcy}}$ with the default choice of $\epsilon_0 = \epsilon$ are substantially smaller in modulus than those for SWs; only for much higher z do the extrema of $\tilde{u}_0^{\text{hcy}}$ approach the SW values which they reach in the infinite-z limit. It is easily checked that these observations also hold in comparison with other short-ranged potentials like, e.g., the Lennard-Jones one: the main difference relative to SWs concerns the phase rather than the amplitude of the oscillations. Taken together, the smallness of the local extrema of $\tilde{\phi}^{\text{hcy}}$ and the *rôle* the temperature plays readily explain the especially attractive numerical properties of this potential. For $Q \to 0$, the slope of $\tilde{u}_0$ relative to the scale set by the oscillations at higher Q is particularly steep, as per Section 3.2 leading to especially small $Q_{\Delta Q}$ and suppression of near-discontinuities of f. At intermediate cutoff, on the other hand, the smallness of the local extrema *vis-à-vis* the global maximum at $Q = 0$ renders the numerics there similar to what would be seen at much higher T/T_c in other systems, and transient stiffness poses less of a problem. At the same time, the z-dependence of $\tilde{u}_0^{\text{hcy}}$ immediately explains the deteriorating accuracy of the results for very short HCY screening length.[13]

Support for this view comes from the numerical properties following from a different choice of $w(r)$ inside the hard core, which affects the Fourier transform $\tilde{\phi}$ and hence f and all other properties of the Q system at all cutoffs except in the limits $Q \to \infty$ and $Q \to 0$. (Independence of the final results from the precise choice of w is confirmed in a rather satisfactory way in some preliminary calculations on the Girifalco description of fullerenes.[14]) The simplest such modification of w consists in a non-default setting of ϵ_0 in Eq. (2), exemplified by the dot-dashed curve in Fig. 4 ($\epsilon_0 = 0$). Just as in ref. 12, even a modest discontinuity of $w(r)$ at $r = \sigma$ strongly affects the form of $\tilde{\phi}$ and renders the local extrema similar to those of the SW case; as expected, this is accompanied by numerical difficulties at intermediate Q similar to those discussed for SWs in refs. 9 and 10. In contrast, extension of the Yukawa form all the way to the origin – hardly unproblematic as it entails diverging direct correlation function at $r = 0$ and invalidates the expansion method of taking into account the core condition[6] – yields the non-oscillatory form $\tilde{u}_0(Q) = z^2/(z^2 + Q^2)$ (dotted curve in Fig. 4) and prevents numerical solution of the FDEs even at high temperatures. The exceptionally attractive numerical properties of

the potential (2) are therefore merely the result of a particular choice, shared with the original implementation, of $w(r)$ inside the core and so no genuine trait of the HCY fluid.

This finding nevertheless does not invalidate the special standing of the HCY system that must be taken into account in interpreting a comparison with other thermodynamically consistent liquid state theories on the basis of HCY results for $1.8/\sigma \leqslant z \leqslant 9/\sigma$.[13] On the other hand, the above considerations also point to the possibility of tuning the computational properties of some given potential by optimizing $w(r)$ inside the core to reduce the local extrema at intermediate cutoff, an avenue largely unexplored to date the merit of which we are currently in no position to assess.

The preceding clarification regarding the HCY system *vis-à-vis* other potentials is but one application of the detailed understanding of the HRT numerics presented here as well as in our earlier HRT related work. Other aspects of the numerics where this understanding has proved invaluable in interpreting the computational process and the results it yields concern the limits of the resolution in ρ when using extremely fine density grids, the interplay between non-uniform discretization grids and the location of the binodal, the local behavior of the solution close to the zeros $Q_{\tilde{\phi},i}$ of $\tilde{\phi}$, or questions of data analysis. All-in-all, we feel that we have amassed a considerable amount of numerical experience and arrived at a rather detailed self-consistent perception of the computational process throughout all of $\mathcal{D}$ even below the critical temperature. Given the precarious nature of the HRT numerics and the not altogether unproblematic relation between the PDE and its FD approximation such an understanding is of prime importance if systematic mistakes are not to be introduced into the results unknowingly.

ACKNOWLEDGMENTS

The authors gratefully acknowledge financial support from *Fonds zur Förderung der wissenschaftlichen Forschung* (*Austrian Science Fund*, FWF) under projects P14371-TPH, P15758-N08 and J2380-N08.

REFERENCES

1. A. Reiner, Infinite compressibility states in the hierarchical reference theory of fluids. I. Analytical considerations, *J. Stat. Phys.* **118**:1107–1127 (2005).
2. A. Parola and L. Reatto, Liquid state theories and critical phenomena, *Adv. Phys.* **44**:211–298 (1995).
3. A. Parola and L. Reatto, Liquid-state theory for critical phenomena, *Phys. Rev. Lett.* **53**:2417–2420 (1984).

4. A. Parola and L. Reatto, Hierarchical reference theory of fluids and the critical point, *Phys. Rev. A* **31**:3309–3322 (1985).
5. A. Parola, A. Meroni and L. Reatto, Comprehensive theory of simple fluids, critical point included, *Phys. Rev. Lett.* **62**:2981–2984 (1989).
6. A. Meroni, A. Parola and L. Reatto, Differential approach to the theory of fluids, *Phys. Rev. A* **42**:6104–6115 (1990).
7. A. Parola, D. Pini and L. Reatto, First-order phase transitions, the Maxwell construction, and the momentum–space renormalization group, *Phys. Rev. E* **48**:3321–3332 (1993).
8. M. Tau, A. Parola, D. Pini and L. Reatto, Differential theory of fluids below the critical temperature: Study of the Lennard-Jones fluid and of a model of C_{60}, *Phys. Rev. E* **52**:2644–2656 (1995).
9. A. Reiner and G. Kahl, Implementation of the hierarchical reference theory for simple one-component fluids, *Phys. Rev. E* **65**:046701 (2002).
10. A. Reiner, The hierarchical reference theory. An application to simple fluids, PhD thesis, Technische Universität Wien (2002). Available from: http://purl.oclc.org/NET/a-reiner/dr-thesis/.
11. A. Reiner, *ar-HRT-1. Implementation of the Hierarchical Reference Theory for one-component fluids.* Available from: http://purl.oclc.org/NET/ar-hrt-1/.
12. A. Reiner and G. Kahl, The hierarchical reference theory as applied to square well fluids of variable range, *J. Chem. Phys.* **117**:4925–4935 (2002).
13. C. Caccamo, G. Pellicane, D. Costa, D. Pini and G. Stell, Thermodynamically self-consistent theories of fluids interacting through short-range forces, *Phys. Rev. E* **60**:5533–5543 (1999).
14. L. A. Girifalco, Interaction potential for C_{60} molecules, *J. Phys. Chem.* **95**:5370–5371 (1991).